PAPER

Evidence for inhibition of HIF-1α prolyl hydroxylase 3 activity by four biologically active tetraazamacrocycles†

Jing Cao, Zhirong Geng, Xiaoyan Ma, Jinghan Wen, Yuxin Yin and Zhilin Wang*

Hypoxia inducible factor 1 (HIF-1) is central to the hypoxic response in mammals. HIF-1α prolyl hydroxylase 3 (PHD3) degrades HIF through the hydroxylation of HIF-1α. Inhibition of PHD3 activity is crucial for up-regulating HIF-1α levels, thereby acting as HIF-dependent diseases therapy. Macrocyclic polyamines which display high stability on iron-chelating may well inhibit the enzyme activity. Thus inhibition and interaction on catalytic PHD3 by four biologically active tetraazamacrocycles (**1–4**), which have two types of parent rings to chelate iron(II) dissimilarly, were studied. The apparent IC_{50} values of 2.56, 1.91, 5.29 and 2.44 μM, respectively, showed good inhibition potency of the four compounds. K_I values were 7.86, 3.69, 1.59 and 2.92 μM for **1–4**, respectively. Different inhibition actions of the two groups of compounds were identified. Circular dichroism (CD) and fluorescence spectrometries proved that one type of compound has significant effects on protein conformation while another type does not. Computational methodology was constructed to employ the equilibrium geometry of enzyme active site with the presence of substrate competitive inhibitor. Iron(II) coordination in the active site by inhibitors of this kind induces conformational change of the enzyme and blocks substrate binding.

Introduction

Hypoxia inducible factor 1 (HIF-1), functioning as a master regulator through of oxygen homeostasis, mediates cellular and physiological responses to changes in dioxygen levels in animals.[1] HIF prolyl hydroxylase 3 (PHD3) catalyzes the hydroxylation of conserved prolyl residues in the HIF-1α subunit under well-oxygenated conditions, which generates HIF proteasomal degradation. Under hypoxic conditions, the PHD3 activity decreases, which blocks the degradation of HIF-1α and activates the transcription of many genes related to oxygen homeostasis.[2,3] PHD3 belongs to the 2-oxoglutarate (2OG)-dependent dioxygenase superfamily,[4] in which iron(II) plays an important role in the catalytic site of the enzyme.[5,6] Many of 2OG dependent dioxygenases bind their iron cofactor *via* a conserved two histidinyl-one aspartyl/glutamyl triad of residues, leaving two positions for binding of 2OG and one for molecular oxygen.[7] Since oxygen-dependent PHD3 negatively regulates HIF-1, inhibition of PHD3 might be beneficial for many diseases related with HIF upregulation.[8,9] To achieve the goal of moderate HIF-dependent processes, small-molecule inhibitors that might inactivate PHD3 activity have drawn the attention of both the academia[10–22] and pharmaceutical campanies.[23]

Reported molecules that inhibit activity of PHDs are from two groups: proline analogues and metal-chelating inhibitors.[13–15] Most iron-coordinating PHD inhibitors are 2OG analogues,[10,11,16–18,24] such as N-oxalylglycine (NOG) and its derivatives,[19,20,25] bicyclic aromatic moleculors,[21] citric acid cycle intermediates,[22] *etc.* Inhibitors of this kind all have simple 2OG similar scaffolds, which bind to the active site iron(II) in a bidentate mode. 2OG analogues are identified as potential 2OG competitive inhibitors through competitively occupying iron(II) binding site of 2OG in enzyme catalytic center to stabilize the level of HIF-1α.[16] Besides, natural iron-chelating compound, desferroxamin mesylate (DFO), is found to inactivate the PHDs activity by iron(II) chelation that decreases the concentration of Fe^{2+} in the enzyme active site, resulting in the upregulation of HIF related gene levels in patients afflicted with chronic disease anemia, rheumatoid arthritis, and neuronal injury.[26] Many studies have provided that DFO increases the stability of HIF-1α at cellular levels.[27–29]

Macrocyclic polyamines are essential for life and participate in a bewildering number of seemingly unrelated processes.[30,31]

State Key Laboratory of Coordination Chemistry, School of Chemistry and Chemical Engineering, Nanjing University, Nanjing 210093, P. R. China. E-mail: wangzl@nju.edu.cn; Fax: +86-25-83317761; Tel: +86-25-83686082

†Electronic supplementary information (ESI) available: Details of activity reaction procedure and preparation of **1–4**, double reciprocal plots for the inhibition of hydroxylation activity by tetraazamacrocycles **1–4**, fluorescence emission spectra of PHD3 with increasing amounts of **1–4**, fluorescence emission spectra of PHD3–Fe^{2+}/PHD3–Fe^{2+}–2OG mixtures with increasing amounts of **1** and **2**, determination of association constant (*Ka*) of **1–4** to Fe^{2+}, computationally optimized energy and coordinates of **4**–Fe^{2+} and residues of first shell of PHD3 active site, selected lengths (Å) and bond angles (°) of the computational model, calculated average log *P* of **1–4**. See DOI: 10.1039/c2ob07076f

These compounds comprise a special group of heterocycles that bind different guests.[32] In some situations they mimic the effects of bio-molecules by competing for the same binding sites on receptors or enzymes.[33] Moreover, many macrocyclic poly-amines and their transition metal complexes have cytotoxic activities to tumors.[34,35] Thus this type of compound has been focused on medical applications. Some of the pioneering work on macrocyclic polyamines has concentrated on potent SOD (superoxide reductase) mimics.[36] Non-heme iron enzymes such as Fe-SOD or PHDs all have non-heme His, Asp ligated active sites.[37–39] As a starting point, we aim to investigate such bio-mimic compounds that may dechelate the metal from biologic chelators or bind iron(II) at the enzyme active site. Polynitrogen compounds were identified to inhibit hydroxylation activity of PHD3, and the inhibition was supposed to be iron(II)-chelating interaction.[40] Macrocyclic polyamines are proved to have higher stability on Fe^{2+} binding due to the cyclic structure.[41] However, few studies have focused on PHDs inhibitors that have macrocyclic polyamine structures so far.

Among the biologically active macrocyclic polyamine series, tetraazamacrocyles have relatively appropriate coordination number and binding affinity to iron(II) in 2OG dependent dioxygenases study. Tighter iron-binding of pentaaza or higher polyaza macrocycles with more nitrogen atoms of the heterocycle may cause irreversible chelation of iron away from the active site. The compounds may have the same inhibition mechanism with natural iron-chelating compounds. But the reversibility of inhibition might be even worse. Besides, higher polyaza macrocycles are not easy to directly interact with the enzyme active site. Our group has strong interests in biological application of tetraazamacrocycles.[35,42] In this paper, considering iron(II)-binding ability, coordination number and inhibition potency, we studied four tetraazamacrocycles (**1**–**4**, Scheme 1) of their inhibition on PHD3 activity. The parent rings of four compounds belong to two different macrocyclic structures. The different side arms were chosen to observe effects of distinct iron(II)-binding mode. In protein–iron(II)-2OG complex center, the four compounds may chelate Fe^{2+} through parent rings and/or groups in side arms, according to their structural differences.
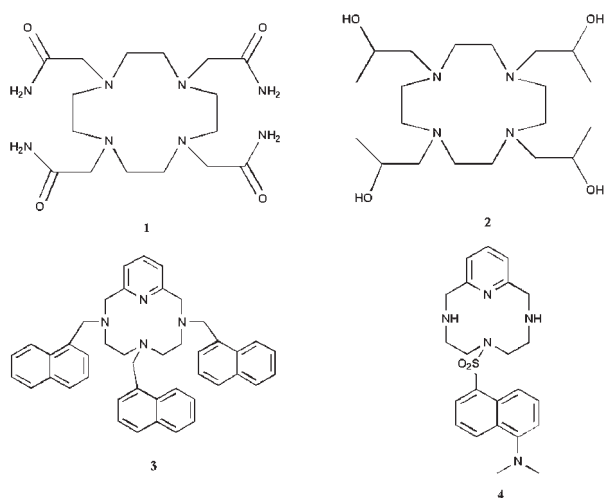
Inhibition kinetics study presented the inhibition action of the four compounds. For more evidence to understand the interactions, spectroscopic methods of circular dichroism (CD) and fluorescence spectrometry were performed. The quantitative analysis of estimation of enzyme secondary structure elements from CD spectra and ligand binding study from protein fluorescence spectra described the effects of tetraazamacrocycles on conformational change and binding affinity of PHD3. Computational methodology was also used to understand the mechanism of inhibition by modeling competitive inhibitor binding to the iron site of the enzyme.

Result and discussion

Expression and purification of recombinant human PHD3

Earlier studies have illustrated that PHD3 aggregated when over-expressed in mammalian cells.[43] The low activity of PHD3 for *E. coli* may also be as a consequence of the aggregation of PHD3 at high protein concentration. PHD3 is the least purified and studied isoenzyme in the PHD family. We purified soluble and active human PHD3 with a few improved procedures based on former studies.[40,43] The purification became more efficient *via* this improvement. A highly reducing condition is a prerequisite for successful purification of the recombinant human PHD3 of high purity, thus DTT is required in all purification procedures to avoid the formation of intermolecular disulfide bonds. The presence of high concentrations of salt (2 M NaCl) is necessary in purification procedures, to avoid protein aggregation in buffers with low salt concentration. Recombinant human PHD3 could hydroxylate the proline of the HIF-1α peptide to form hydroxyproline *in vitro*. As described previously,[40] a mass increase of 16 Da of the resultant peptide product verified that the proline residue of HIF 19 peptide was hydroxylated and the purified enzyme was catalytic.

Kinetics study of HIF PHD3

Quantitative analysis of the kinetic properties was carried out. The HPLC method used in a former study[40] was time-consuming, so we used a reported detection method based on derivatization of 2OG by using *o*-phenylenediamine (OPD) to give a fluorescent product.[44] The rate of 2OG decarboxylation was estimated by fitting the Michaelis–Menten equation (eqn (1))

$$V = [S]V_{max}/(K_M + [S]) \qquad (1)$$

where V is the initial velocity of the reaction, percentage of consumed 2OG (2OG consumed% min^{-1}), [S] the substrate (HIF-1α peptide) concentration (μM), V_{max} the maximal velocity of the reaction (2OG consumed% min^{-1}), and K_M the Michaelis constant for HIF-1α peptide (μM). The kinetic parameters of apparent K_M and V_{max} values were 3.6 ± 1.4 μM and 1.33% ± 0.14% min^{-1} by fitting the nonlinear regression (Fig. 1a). As Lineweaver–Burk plot is widely used to determine the apparent K_M, double reciprocal plot of the relation between the concentration of the substrate and the rate was fitted to verify the result from nonlinear curve fitting. Consistent results of apparent K_M and V_{max} values were given of 2.9 ± 0.4 μM and

Scheme 1 Structure formulae of compounds 1–4.

3914 | *Org. Biomol. Chem.*, 2012, **10**, 3913–3923

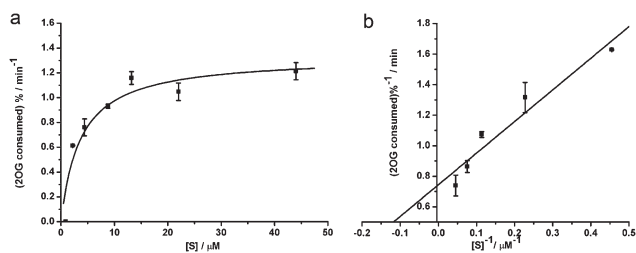This journal is © The Royal Society of Chemistry 2012

Fig. 1 Enzyme kinetics of HIF PHD3. (a) Substrate concentration dependence of rate (represented by percentage of 2OG consumption per min). Values of kinetics parameters were estimated by direct fitting of the Michaelis–Menten equation. (b) Double reciprocal plots of the relation between the concentration of peptide substrate and the initial velocity. The enzyme concentration was 5 μg. Data were analyzed as mean ± S.D. of three independent experiments.

$1.34\% \pm 0.13\%$ min^{-1}. The experimental points were quoted as a mean of three independent measurements (Fig. 1b).

The initial velocity of the reaction was represented by the percentage of consumed 2OG during the reaction time of 20 min. The normalization of 2OG consumption is a way to contrast the data produced by different detection times. The kinetic parameter values of PHD3 have not been determined by using the fluorescence derivatization assay before. And our new result of K_M value of PHD3 for peptide substrate is similar to other prolyl hydroxylases (PHD1, 7 μM and PHD2, 4 μM).[44] The fluorescence-based assay has been used to study the kinetic parameters of 2OG dependent oxygenases such as FIH and PHD2.[44] We used this procedure to study not only the kinetics of PHD3 but also inhibition of the enzyme activity by tetraazamacrocycles. The inhibition types of the four molecules were characterized via this method as well.

The inhibition of the recombinant human PHD3 activity by tetraazamacrocycles 1–4

Respecting that PHD isozymes play an integral role in oxygen homeostasis, inhibition of the HIF-1α PHD3 activity is attractive from the perspective of developing pharmaceuticals for diseases.[8,9] Polynitrogen compounds had been identified to inhibit hydroxylation activity of PHD3, and the inhibition was supposed to be an iron(II)-chelating interaction.[40] Macrocyclic polyamines are cyclic polynitrogen compounds that have higher stability on Fe^{2+} binding due to their cyclic structure. Four tetraazamacrocycles (**1–4**) (Scheme 1) have been studied the inhibition of PHD3 activity. The association constant (K_a) values of the four compounds binding to iron(II) are 1.08×10^4 M^{-1}, 1.19×10^4 M^{-1}, 5.05×10^5 M^{-1}, 4.45×10^5 M^{-1}, respectively (Fig. S4†). The K_a values are much higher than the non-cyclic compounds studied before. It was proposed that tighter binding with iron(II) caused lower IC$_{50}$ values, thus the four cyclic compounds might be relatively better PHD3 inhibitors. In addition, **3** and **4** displayed tighter coordination than **1** and **2**. It was attractive for us to understand the relationship between iron(II) binding affinity and inhibition actions of the small molecules. The macrocyclic scaffolds have been designed with the goal of discovering structurally diverse PHD3 inhibitors. The structures of four compounds are shown in Scheme 1. The parent rings of
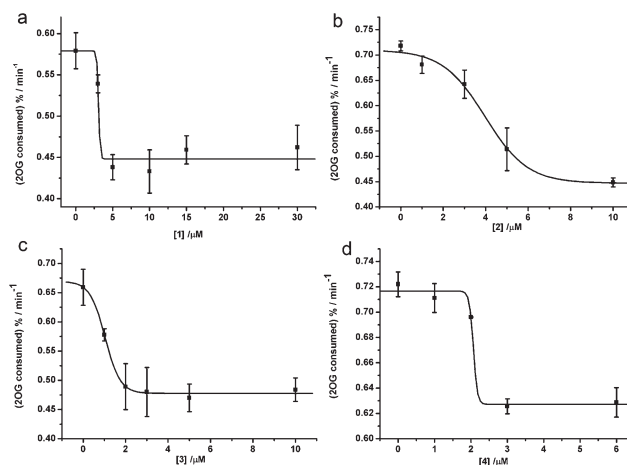

Fig. 2 Effects of tetraazamacrocycles (a) **1**, (b) **2**, (c) **3**, (d) **4** on the hydroxylation activity of PHD3. Incubations were carried out at the K_M of HIF-1α peptide substrate and saturating concentration of 2OG, with increasing amounts of compounds (0–30 μM). IC$_{50}$ values were estimated by dose regression of initial velocity versus concentration of tetraazamacrocycles. The data was analyzed as mean ± S.D. of three independent experiments.

Table 1 Biological activity of **1–4** against PHD3 determined by using the fluorescence derivatization assay

Inhibitors	IC$_{50}$/μM	K_I/μM
1	3.09	9.98
2	3.97	6.28
3	1.03	1.91
4	2.07	2.49

four compounds belong to two different tetraazamacrocycle series, which provide two types of Fe^{2+} coordination mode. Compounds **1** or **2** chelates Fe^{2+} in a hexacoordinative mode through four nitrogens of the macrocycle and two oxygens in side arms, as indicated by the crystal structure of complex of compound **1** and **2** coordination with Zn(II)[37,38] and Mn(II).[45,46] However, earlier crystal structures of iron(II) complexes using parent ring of **3** and **4** as ligand implied that they tend to coordinate Fe^{2+} via triad or tetrad from nitrogen atoms of the parent ring (CCDC reference numbers 639153 and 628570), which leaves vacant position for other ligands binding. Correlation between binding mode and inhibition action drove us to explore the effects of the four tetraazamacrocycles on the function of PHD3. It was believed that the properties of side arms might also effect the interactions with amino acid residues of the protein.

The four compounds inhibit the enzyme catalytic activity in a concentration-dependent , and the IC$_{50}$ values were estimated at a variety of concentrations of inhibitors. The known K_M value was used as peptide substrate concentration. Effects of the small molecules on the detection of product fluorescence were premeasured, which proved that the impacts could be neglected up to the highest concentrations of the compounds used in the assay procedure. Fig. 2 showed the dose-response regression of initial velocity versus concentration of tetraazamacrocycles. The apparent IC$_{50}$ values of **1–4** are 3.09, 3.97, 1.03 and 2.07 μM,

respectively (Table 1). The values above implied that the four compounds all displayed relatively good inhibition activity, compared with non-cyclic polynitrogen compounds studied before. The IC_{50} values of **1** and **2** were slightly greater than that for **3** and **4**, though this difference was not statistically significant. The result suggested that iron(II) binding affinity correlates to inhibitory potency.

Knowledge of inhibition action might help to improve the structure-guided design and develop a novel series of PHD inhibitors, which target for HIF up-regulating dependent diseases therapy. The kinetics analysis characterized the inhibition of PHD3 activity by these compounds over a range of HIF-1α peptide concentrations from 10^{-6} M to 10^{-5} M. Global fitting of the Michaelis–Menten equation have provided the inhibition type of tetraazamacrocycles (Fig. 3). Double-reciprocal ($1/V$ versus $1/$[HIF-1α peptide]) plots have been used as supplements (Fig. S1†). Both non-linear and linear fitting indicates that the inhibition types of two groups of compounds are different. With the increasing amounts of **1** and **2** in enzyme activity assay, the maximal velocity (V_{max}) of the reaction declined and the apparent Michaelis constant (K_M) was approximately equivalent to the actual Michaelis constant (Fig. 3a, 3b and Fig. S1a, S1b†). However, the value of V_{max} of the reaction was nearly unchanged and the apparent K_M increased with the increasing of **3** and **4** (Fig. 3c, 3d and Fig. S1c, S1d†). The K_I values of 9.98, 6.28, 1.91, 2.49 μM were obtained from the replot of the slopes of the corresponding double-reciprocal plots versus concentration of tetraazamacrocycles **1–4**[47] (Table 1). The results showed that the inhibition of **1** and **2** is inclined to be noncompetitive, whereas **3** and **4** are competitive inhibitors of the substrate, **3** is not typically substrate competitive. The reason might be attributed to some interactions between bulky pendant arms and hydrophobic residues of the enzyme or substrate. The K_I values suggested that

tighter binding of the competitive inhibitors to the enzyme catalytic site.

The relationship of PHD3 activity inhibition and iron chelation caused by **1–4** was further discussed. The over-dosing of Fe^{2+} after inhibition reaction was performed. The four inhibitors were individually added into the reaction tubes, containing the same reaction mixture as enzyme activity assay described in the experimental section. After incubation of reaction mixtures at 37 °C for 20 min, additional Fe^{2+} was added into the reaction mixtures and the incubation was continued for another 20 min. The regular activity assay without inhibitors was carried out as control. For comparing with the 2OG consumption of four reaction mixtures and the control group, the regular inhibition assays of **1–4** were referred to the dose-response curve of Fig. 2. The level of inhibition was basically reversed after overdosing of Fe^{2+} (Fig. 4). Therefore, a conclusion can be given that the inhibition of enzyme activity from tetraazamacrocycles are reversible and Fe^{2+} relevant. The results proved the previous speculation that the decrease of catalytic activity is due to the coordination interactions of these compounds with iron(II).[40]

The results above verified the hypothesis that iron(II) coordination contributed to dissimilar modes on inhibition of PHD3 activity. According to the data, we proposed some rational assumptions to explain the effects. The noncompetitive inhibitors do not directly affect the catalytic center of the enzyme by the reason that a six-coordinate iron(II) complex is uncapable to react with other ligands. The inactivation of enzyme activity by **1** or **2** is attributed to the decrease of iron(II) concentration by inhibitor coordination. In contrast, the competitive inhibitors **3** and **4** have direct effects on the Fe^{2+} of catalytic center, or some other interactions with the enzyme or peptide substrate in active pocket. Details of these effects should be further investigated by spectroscopic methods on protein–iron(II)-inhibitor interaction.
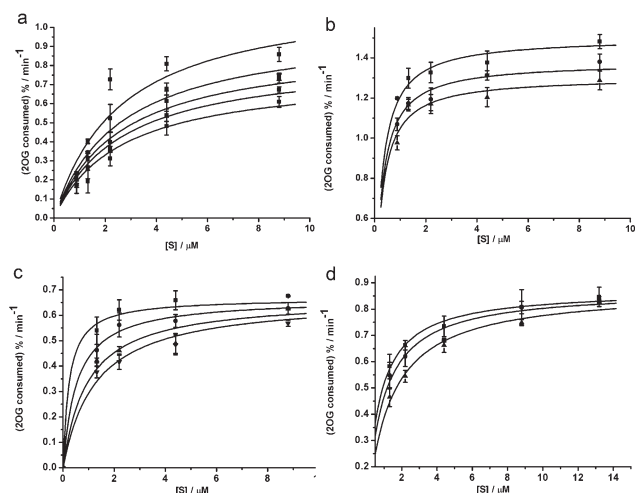

Fig. 3 Concentration dependence of rate for the inhibition of PHD3 activity by compound **1–4**. The data were analyzed by global fitting of the Michaelis–Menten equation. (a) Plots for **1** concentration of 0 μM (■), 1 μM (●), 3 μM (▲), 5 μM (▼) and 10 μM (◆). (b) Plots for **2** concentration of 0 μM (■), 3 μM (●) and 5 μM (▲). (c) Plots for **3** concentration of 0 μM (■), 1 μM (●), 2 μM (▲), 10 μM (▼). (d) Plots for **4** concentration of 0 μM (■), 1 μM (●) and 2 μM (▲). The data was analyzed as mean ± S.D. of three independent experiments.

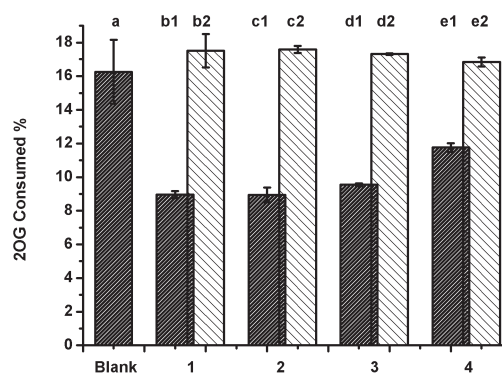**Fig. 4** Effects of Fe^{2+} over titration on the inhibition of PHD3 by **1–4**. The effects were tested by over-titration of 50 μM Fe^{2+} after inhibition assay by **1–4**. The consumption ratio of 2OG is nearly 16–17%, but decreases to 9–11% with inhibitors existing, and the activity of enzyme is basically recovered after overdosing of Fe^{2+}. (a) Control. The reaction mixture was incubated with absence of inhibitors and over-titrated Fe^{2+} after 20 min of normal assay. (b1, c1, d1, e1) Ratio of consumed 2OG in inhibition assays by **1–4**. The data was referred to Fig. 2. (b2, c2, d2, e2) Over-titration of Fe^{2+} after assay b1, c1, d1 and e1. All tubes of reaction mixtures with inhibitors were incubated for 20 min at 37 °C. After additional 50 μM of Fe^{2+} was added into the reaction tubes, the incubation was continued for another 20 min. The data was analyzed as mean ± S.D. of three independent experiments.

3916 | *Org. Biomol. Chem.*, 2012, **10**, 3913–3923

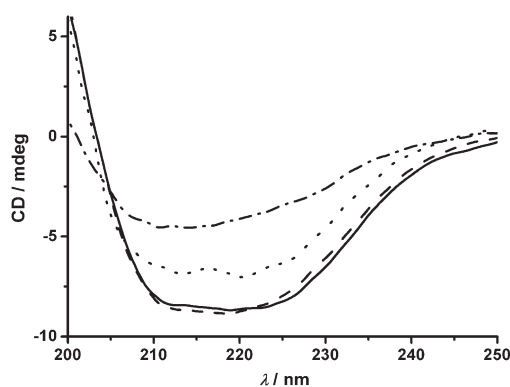This journal is © The Royal Society of Chemistry 2012

Fig. 5 CD spectra of PHD3 in the absence and presence of cofactors and peptide substrate. The spectra were taken at the protein concentration of 4 μM. PHD3: solid line; PHD3–Fe²⁺: dashed line; PHD3–Fe²⁺–2OG: dotted line; PHD3–Fe²⁺–NOG-substrate: dash dotted line (2OG was displaced by NOG to avoid the hydroxylation reaction).

Table 2 Estimated secondary structures of PHD3, PHD3–Fe²⁺, PHD3–Fe²⁺–2OG and PHD3–Fe²⁺–2OG -HIF-1α peptide substrate mixtures from CD spectra

Samples	α (%)	β (%)
PHD3[a]	51.17 ± 1.31	33.11 ± 1.06
PHD3–Fe²⁺[b]	52.88 ± 1.19	31.73 ± 0.91
PHD3–Fe²⁺–2OG[c]	59.00 ± 1.30	26.77 ± 1.05
PHD3–Fe²⁺–NOG[c]–HIF-1α[d]	40.87 ± 0.26	41.44 ± 0.21

Values represented the mean ± S.D. of three independent experiments. [a] Spectra were taken at the protein concentration of 4 μM. [b] Concentration of Fe²⁺ was 50 μM. [c] Concentration of 2OG and NOG was 500 μM. [d] Concentration of HIF-1α 19 mer was 10 μM.

CD spectra study and secondary structure analysis of PHD3

Effects of cofactors and inhibitors on conformational change of PHD3 remains unclear because of difficulties in purification and crystallization the recombinant human PHD3. CD spectrometry is a sensitive method to analyze protein secondary structure in solution.[48] We used CD spectra successfully characterized the recombinant PHD3 within the wavelength range of 200–250 nm. In this data range, α-helix is generally the only secondary structure that can be determined with confidence.[49] The content of α-helix was estimated with the Jasco secondary structure manager software using the reference CD data-Yang. Jwr.[50] and an empirical equation between α-helix and β-sheet contents provided an estimate of β-sheet as reported previously.[50,51] The PHD3 was analyzed to have the secondary structures of 51.2% α-helix and 33.1% β-sheet in 37 °C (Fig. 5 solid line). Estimation of PHD3 secondary structures provides useful insight into the understanding of small molecules effects on the enzyme conformational change.

Fig. 5 and Table 2 showed CD spectra and the calculation of secondary structure elements of PHD3 in the absence and presence of cofactors and substrate. The conformational change of PHD3 was barely noticeable after Fe²⁺ titration, while evident alternation of secondary structures occurred by adding both Fe²⁺ and 2OG, suggesting that the active site of PHD3 has to be stabilized by the formation of PHD3–Fe²⁺–2OG complex. 2OG was displaced by NOG to avoid hydroxylation reaction when HIF-1α peptide was added.[52] The secondary structures of PHD3–Fe²⁺–2OG and PHD3–Fe²⁺–NOG complex are about the equal according to the experimental data (data not shown). Remarkable reduction of helical content and increase of β-sheet suggested that substrate participation results in conspicuous alterations of PHD3–Fe²⁺–NOG complex conformation. In respect that the mobile β2β3/loop of the enzyme in the "closed" position is of significant importance for 2OG/inhibitor and HIF-α substrate binding,[52] the high level of β-sheet content reflected that the enzyme was catalytically active. The effect is compatible with previous study of catalytic domain of PHD2 in complex with a peptide representing its HIF-1α CODD substrate, which reveals that a significant conformational change likely occurs concomitant with HIF-α binding.[52]

Earlier research reported that 2OG or analogous inhibitors stabilized catalytic center of 2OG oxygenases,[53,54] so competitive inhibitors interacted with the catalytic domain of the enzyme so would cause conformational change of the enzyme. The direct evidence is to investigate the effect of these inhibitors on the secondary structures of PHD3. The inhibitors **1–4** were titrated individually into PHD3, PHD3–Fe²⁺ and PHD3–Fe²⁺–2OG complex, and the CD spectra of mixtures were recorded. No significant differences in secondary structure elements of PHD3 were observed with addition of **1–4**, though distinctions can be seen between the samples with and without inhibitors (Fig. 6a a1–a5). Remarkable gain of PHD3 helical content occurred with titration of inhibitor **3** or **4** in presence of Fe²⁺, concomitant with a transient loss of β-sheet content (Fig. 6a b4, b5). 2OG was then individually titrated into four mixtures in the presence of enzyme, Fe²⁺ and inhibitors, in which a sharp reduction of helical content and increase of β-sheet were discovered by effects of inhibitor **3** or **4** (Fig. 6a c4, c5). Only slight changes in secondary structure elements were found in PHD3–Fe²⁺/PHD3–Fe²⁺–2OG mixtures with the presence of inhibitors **1** or **2** (Fig. 6a b2, b3, c2, c3), which was because that iron(II)-chelation decreases the amounts of PHD3–Fe²⁺–2OG complex, but the interaction only has weak effects on the active site of PHD3. Distinctions of effects on CD spectra by two kinds of inhibitors are notable. Consistent results were obtained for PHD3–Fe²⁺–2OG complex in the presence of HIF-1α peptide substrate, the conformation of the mixtures changed more evidently after titration **3** and **4** (Fig. 6b). The data confirmed the fact that the effects of **3** or **4** on PHD3 are Fe²⁺ dependent. It seems that formation of PHD3–Fe²⁺-inhibitor complex causes enzyme conformational change. And it was confirmed that 2OG has ability to bind Fe²⁺ in the active site after inhibitor coordination. These results strongly support the kinetics study that inhibition is categorized into two types, and the competitive inhibitors do interact on the catalytic center of PHD3 and induce conformational change of the enzyme.

PHD3   fluorescence spectra analysis

Fluorescence spectrometry was carried out to study the effects of inhibitors **1–4** on fluorescence of PHD3/PHD3–Fe²⁺/PHD3–Fe²⁺–2OG mixtures. **1–4** have little effect on the
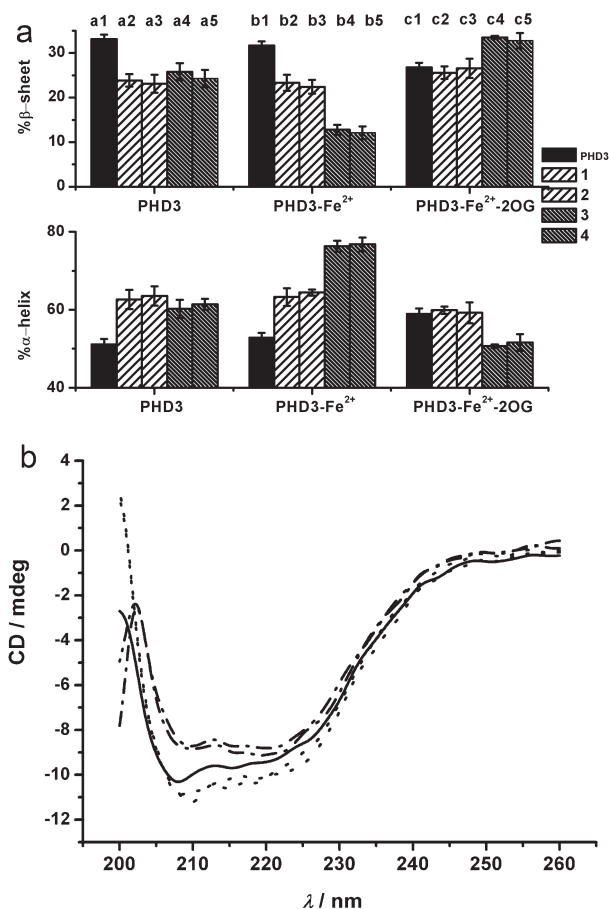
Fig. 6 Effects of tetraazamacrocycles **1–4** on the conformational change of PHD3 with absence and presence of co-factors and substrates. (a) Estimation of secondary structure contents of PHD3/PHD3–Fe^{2+}/PHD3–Fe^{2+}–2OG mixtures affected by **1–4**. (a1) Control 1, the sample contained 4 μM PHD3. (a2–a5) Samples same as control 1 were added with 50 μM tetraazamacrocycles **1–4**, respectively. (b1) Control 2, the sample contained 4 μM PHD3 and 50 μM Fe^{2+}. (b2–b5) Samples from a2–a5 were added with 50 μM Fe^{2+}. (c1) Control 3, the sample contained 4 μM PHD3, 50 μM Fe^{2+} and 160 μM 2OG. (c2–c5) Samples from (b2–b5) were added with 160 μM 2OG. The data was analyzed as mean ± S.D. of at least two independent experiments. (b) Contrast of the CD spectra of enzyme–Fe^{2+}–2OG-substrate mixture (solid line) and the conformational change with the addition of 50 μM **1** and **2** (dotted line), and **3** and **4** (dash dotted line). The CD spectra were taken at room temperature with the samples pre-incubated at 37 °C.

fluorescence of the enzyme with absence of Fe^{2+} (Fig. S2†). No significant trends of fluorescence changes were observed in PHD3–Fe^{2+}-**1/2** mixture (Fig. S3a, S3b), whereas **3** and **4** quenched the fluorescence of PHD3–Fe^{2+} continually and evidently (Fig. 7a, 7b inset). In addition, the λ_{max} shifted to longer wavelengths with the increasing amounts of compound **3** and **4** (Fig. 7a, 7b). The protein fluorescence quenching data of **3** and **4** binding was then analyzed in terms of Hill equation (eqn (2)).

$$\gamma = [L_f]^n / (K_d^n + [L_f]^n) \qquad (2)$$

where γ is the ratio of the concentration of bound ligand to total available binding sites, $[L_f]$ is the free ligand concentration, K_d is the dissociation constant for the complex of enzyme–Fe^{2+} and
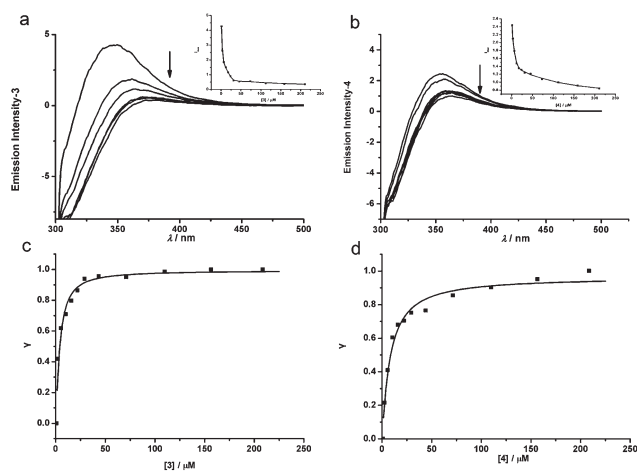

Fig. 7 Fluorescence quenching of **3** and **4** on PHD3–Fe^{2+} mixture. (a) and (b) Fluorescence emission spectra of PHD3–Fe^{2+} mixtures with increasing amounts of **3** (a) and **4** (b) in 50 mM PBS (pH 7.0) at 37 °C. 4 μM PHD3 and 50 μM Fe^{2+} were pre-mixed. Arrows indicated the change in fluorescence intensity upon increasing amounts of ligands. λ (excitation) was 280 nm and maximum λ (emission) shifted to longer wavelengths with ligand binding. Inset: Fluorescence quenching effects of **3** (a) and **4** (b) on the maximum fluorescence emission intensity of PHD3–Fe^{2+} mixture. (c) and (d) Hill plots of the fluorescence quenching data. Experimental data of **3** (c) and **4** (d) binding to PHD3–Fe^{2+} was well fitted by the Hill equation with Hill coefficient (n) of 1.23 and 1.08, respectively.

ligand, and n is hill coefficient.[55] The fluorescence quenching data fitted well through non-linear regression of Hill equation (Fig. 7c, 7d). The average apparent dissociation constant (K_d) values of protein–Fe^{2+} complex binding with **3** and **4** are 5.50 and 9.60 μM, respectively. The Hill coefficient n was estimated to be 1.23 and 1.08, respectively, for **3** and **4** binding to PHD3–Fe^{2+} complex.

The effects of inhibitors on the fluorescence of PHD3–Fe^{2+}–2OG complex were then studied. The fluorescence emission intensity of the complex displayed irregular trend with the titration of **1** or **2** (Fig. S3c, S3d†), while evident quenching effects were observed with the addition of **3** or **4** (Fig. 8 inset). Hill blot provides the average apparent dissociation constant (K_d) values of PHD3–Fe^{2+}–2OG-inhibitor complex (Fig. 8c, 8d). The K_d values are 38.3 and 48.6 μM, respectively, for **3** and **4** binding to PHD3–Fe^{2+}–2OG complex. In addition, weak blue shifts of maximum fluorescence emission wavelengths were observed with the increasing amount of compound **3** and **4** (Fig. 8a, 8b). It was found that the fluorescence of **3** and **4** had no appreciable effect up to the highest concentrations used in the fluorescence quenching experiment. And impacts caused by inhibitors were subtracted by blank groups, in which deionized water contained same concentrations of inhibitors as all PHD3–Fe^{2+}-inhibitor/PHD3–Fe^{2+}–2OG-inhibitor samples.

Fluorescence quenching technique can reveal the nature of binding reaction by the changes found in the fluorescence properties of chromophore.[56] The decrease in fluorescence intensity is attributed to changes in the micro environment of the protein fluorophores caused by binding of the ligand. Trp λ_{max} is quite sensitive to its local environment and wavelength shift is due to
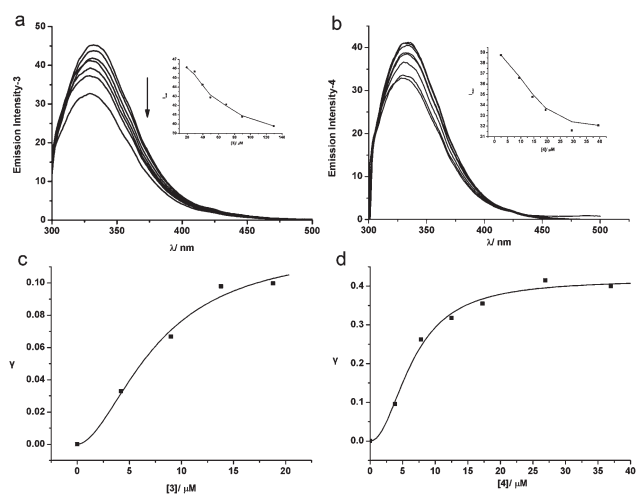
Fig. 8 Fluorescence quenching of **3** and **4** on PHD3–Fe^{2+}–2OG complex. (a) and (b) Fluorescence emission spectra of PHD3–Fe^{2+}–2OG complexes with increasing amounts of **3** (a) and **4** (b) in 50 mM PBS (pH 7.0) at 37 °C. 6 μM PHD3 and 50 μM Fe^{2+} were pre-mixed. Arrows indicated the change in fluorescence intensity upon increasing amounts of ligands. λ (excitation) was 280 nm. Weak blue shifts of the maximum emission wavelengths from the spectra were observed with the increasing of **3** and **4**. Inset: Fluorescence quenching effects of **3** (a), **4** (b) on the maximum fluorescence emission intensity of PHD3–Fe^{2+}–2OG complex. (c) and (d) Hill plots of the fluorescence quenching data. Experimental data of **3** (c) and **4** (d) binding to PHD3–Fe^{2+}–2OG complexes was fitted by the Hill equation with Hill coefficient (n) of 1.80 and 2.06, respectively.

the electric field imposed by the protein and solent.[56] The quenching and λ_{max} shift effects caused by **3** and **4** indicated that conformational change associates with inhibitors binding to iron in the protein active site. It was reported that charged amino acid residue (Lys, Arg, Asp, Glu and any N- or C-terminal residue) and neutral side chains of Asn and Gln makes large contribution to Trp λ_{max} shift.[56] The catalytic center of proly hydroxylases has two His and one Asp binding to the Fe^{2+}. Addition of **3** and **4** might affect the binding site of these amino acid residues, which contributed to the microenvironment alteration around the tryptophans of enzyme catalytic center, and then induced the shift of λ_{max}. The fluorescence quenching effects and the shifts of Trp maximum wavelength have implied that ligand **3** or **4** binding to PHD3 activity center leads to a conformational change of the enzyme, which is consistent with the results of CD spectrometry. The K_d data showed that strong ligand binding occurs when **3** or **4** coordinates to the protein–Fe^{2+} complex. The binding abilities of inhibitor-Fe^{2+} and inhibitor-Fe^{2+}–PHD3 complex are almost at the same level and slightly stronger than PHD3–Fe^{2+}–2OG-inhibitor complex. In another word, there are equilibriums existing, in which **3** or **4** binds simultaneously to PHD3–Fe^{2+}–2OG, PHD3–Fe^{2+} complex and dissociative Fe^{2+}. Inhibitors **1** and **2** do not cause continuous quenching of the protein–Fe^{2+} complex, but still disturb the protein fluorescence. It might be that the inhibitors **1** and **2** decrease the concentration of PHD3–Fe^{2+} complex through Fe^{2+} chelation. Combined with the inhibition kinetics study, it was deduced that competitive inhibitors **3** and **4** could bind to the catalytic center of PHD3. The coordination interactions between inhibitors and active site
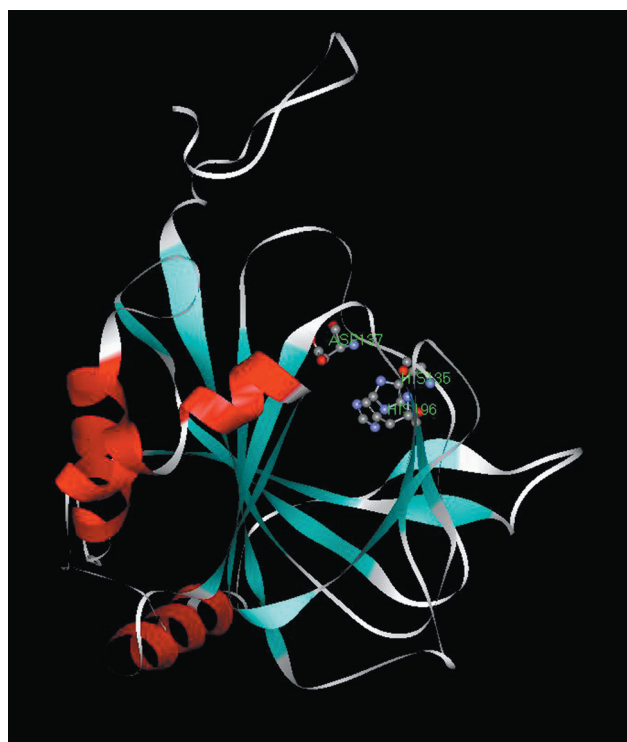

Fig. 9 3D structural model of PHD3 through Swiss-model Server. The model was optimized using the sequence of PHD3 and based on the crystal structures of another PHD isoenzyme–PHD2 (PDB ID: 2HBT). The catalytic domain of the enzyme is from $PHD3_{116}$ to $PHD3_{214}$ as indicated by sequence alignment between PHD3 and its isozymes. The metal binding residues of His_{135}, His_{196} and Asp_{137} were labeled and colored by element.

of PHD3 changed micro environment of the protein, which contributed to conformational change of PHD3. The above studies by CD spectrometry revealed that compound with backbone structure like **3** and **4** might interact with the protein catalytic center. The fluorescence spectrometry reconfirmed the argument. However, the binding mechanism of inhibitors **3** and **4** on the PHD3 active site is still unknown.

Computation of competitive inhibitors binding mode

Tertiary structure of human PHD3 was estimated from the website[57–59] (Fig. 9). The computation automatically simulated PHD3 structure based on the crystal structures of catalytic domain of PHD2.[21] Therefore, starting from the relevant crystal structure (PDB ID: 2HBT), and displacing the inhibitor, composed of the iron(II) ion, side chains of two His and Asp residues, a simplified model was constructed. Such a choice was motivated by the intention to saturate the first ligand shell of the metal in and to keep the smallest size of the system. Theoretical calculations were executed to clarify the coordination geometry of **4**-PHD3–Fe. Equilibrium geometry configurations have been fully optimized using the B3LYP methodology and a slightly modified LANL2DZ basis set. Therefore, the optimized structure is shown in Fig. 10a, in which **4** binds to iron in a tridentate mode. The lone pair electrons on N1, N2 and N4 turned toward
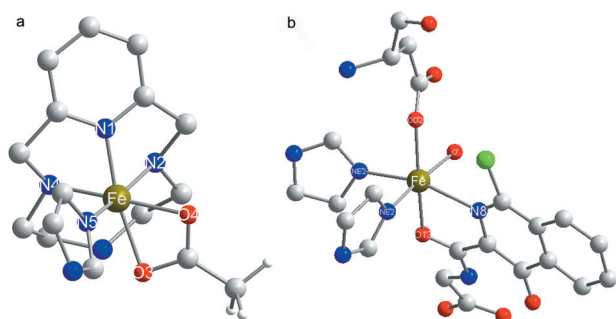
Fig. 10 (a) Optimized geometry of **4**-iron complex with residues of the first coordination shell of PHDs calculated with DFT method. (b) The X-ray structure (2HBT) of the active site of PHD2.

bound iron. Besides, one of imidazole ring deviated from the active site, while N5 from another imidazole ring and O3, O4 from acetic acid was still close to iron ion. The calculated iron–nitrogen bond distances (Fe–N1 = 1.91 Å, Fe–N2 = 2.06 Å, Fe–N4 = 2.06 Å, Fe–N5 = 2.05 Å) and iron–oxygen bond distances (Fe–O3 = 2.07 Å, Fe–O4 = 2.10 Å) are within the average bond distances of Fe–N/Fe–O in iron(II) complexes and 2OG dependent enzymes.[60,61]

Previous studies on crystal structure of functional mimic of 2OG dependent iron(II) dioxygenases revealed a six-coordinate iron center with a one tridentate ligand and bidentate α-keto acid, which suggested that ligands with three nitrogen for coordination are able to binding with iron and leave other binding site vacant to 2OG and dioxygen. For the sake of comparison, the first coordination shell of iron(II) in PHD2 crystal structure (PDB ID: 2HBT) and our computational model are shown together (Fig. 10). By contrasting bond distances and angles, the bidentate acetic acid in equilibrium geometry is likely to replace the site of 2OG analogue instead of Asp residue. **4** provides three nitrogen atoms for iron-chelation, and the remaining three coordination positions are able to be occupied by 2OG and nitrogen from one His residue of the enzyme, suggesting that Asp and another His residues of PHD3 have deviated from iron. In light of coordination mode in the first coordination shell of iron(II) in the computational model, it seems reasonable to assume that significant conformational changes occurs with **4** binding to the active site of PHD3, which is in accordance with the fluorescence and CD spectra changes of PHD3 after **4** binding to the active site. Studies and model systems have indicated that the geometry of 2His–1Asp–2OG–Fe^{2+} complex provides efficient dioxygen binding, and the C–H bond of the substrate points in the direction of the putative dioxygen binding site,[62,63] however, the coordination mode of the active site in our calculation, is incapable of reacting with dioxygen, thereby influences the substrate-binding geometry (Scheme 2). Thus **3** and **4**, which have the same macrocycle to coordinate with iron(II), are thought to be indirectly competitive inhibitors of the substrate.

The mechanism of the active site of HIF hydroxylases is widely acknowledged to form the Fe^{2+}–enzyme–2OG complex in an octahedral geometry.[1] Previously studied bicyclic aromatic metal chelating PHD inhibitors, which bind to the PHDs *via* the oxygen of amide carbonyl and nitrogen of isoquinoline ring, chelate the metal and hinder substrate binding in the closed
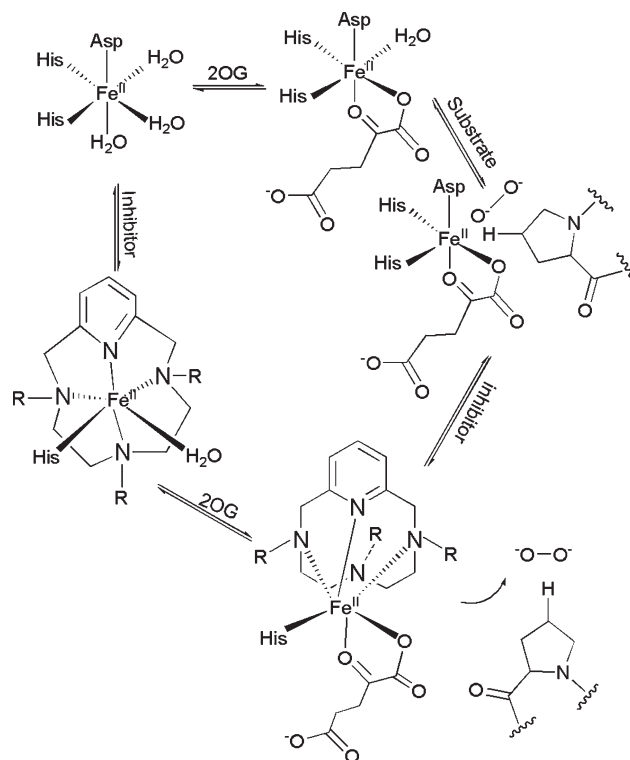
Scheme 2 Proposed inhibition mechanism of **3** and **4**. R is H atom or pendant arms of **3** or **4**.

position.[21,52] In this study, since the chelating interactions are the cause of the decrease of hydroxylation activity, and the differences of inhibition actions are proved to be divided by macrocycle structures, it is supposed that different ways of binding iron(II) by the two types of inhibitors are the reason for dissimilar effects. The chelation of **3** and **4** with Fe^{2+} occupies the coordination position of dioxygen, which disturbs substrate binding by changing the specific conformation of the protein, resulting in the decrease of hydroxylation activity. The inhibition mechanism of **3** and **4** is unique to previously reported PHD inhibitors.

Conclusions

In summary, we studied effects of four biologically active tetraazamacrocycles on the activity of purified recombinant human HIF-1α PHD3. The inhibition types of four tetraazamacrocycles on enzyme activity are dissimilar, distinguished by two kinds of parent rings. Compound **1** and **2** have no significant effect on the conformation of the enzyme. In contrast, the evident alteration of PHD3 conformation is due to the formation of both **3**/**4**–Fe–PHD3 and **3**/**4**–Fe–2OG–PHD3 complexes. Chelation between Fe^{2+} at enzyme active site and nitrogen atoms from the parent ring of **3**/**4** alters the conformation and inhibits the activity of PHD3. The mechanism of inhibiting PHD3 by compounds **1**, **2** is the same as natural iron-chelating compounds such as desferroxamin mesylate (DFO). Their coordination to iron(II) decreases Fe^{2+} concentration in the enzyme active site without influencing the enzyme structure. However, compounds **3** and **4** have different inhibition mechanism from previously reported inhibitors.

These compounds coordinate with Fe^{2+} in the enzyme catalytic center, which changes the conformation of the protein. Unlike the 2OG analogues, **3** and **4** do not occupy the 2OG binding site but the position of dioxygen, which blocks HIF-1α substrate binding, resulting in the decrease of hydroxylation activity. The PHD3 inhibition mechanism of tetraazamacrocycles, which has never been discussed before, provides guidance for effectively developing and synthesizing of potent macrocyclic polyamine inhibitors on the activity of HIF-1α PHD3.

Experimental

General

Expression host, *E. coli* BL21 (DE3) pLysS, and pET32α (+) vector were obtained from Novagen. Isopropyl β-D-thiogalacto-pyranoside (IPTG), 2-oxoglutarate, ascorbate, bovine serum albumin (BSA), dithiothreitol (DTT) and catalase were from Sigma. HIF-1α peptide corresponding to residues 556–574 (DLDLEMLAPYIPMDDDFQL) was sythesized by Shanghai Apeptide Co., Ltd. BCA Protein Assay Kit was from KeyGEN BioTECH. All other reagents were of analytical grade and all solutions were prepared using Milli-Q deionized water. Compounds **1** and **2** were synthesized in our group as reported by Hancock and co-workers.[64,65] **3** and **4** were synthesized as previously reported.[35,42]

Protein expression and purification

The recombinant human PHD3 enzyme was expressed in *E. coli* as described previously.[40] Improvement was made in the purification procedure. The cultured cells were centrifuged at 12 000 rpm for 5 min at 4 °C, each gram of cell pellet was resuspended in 5–10 mL binding buffer (20 mM Na_2HPO_4, 2 M NaCl, 5 mM imidazole, pH 7.0), followed by sonication on ice and centrifugation at 14 000 rpm for 10 min. The supernatant was filtered through 0.45 μm hydrophilic polypropylene membrane to prevent clogging of the chromatography medium. HisTrap FF crude column was pre-equilibrated with 3 column volumes of binding buffer. The extract was applied to the column at 3 mL min^{-1} and flow through was collected for analysis. The column was then washed with 5 column volumes of binding buffer at 3 mL min^{-1} followed by 10 column volumes of washing buffer containing 100 mM imidazole (otherwise identical to binding buffer) at 3 mL min^{-1}. When absorption was back to the base line, target proteins were eluted with a linear gradient from 100 to 500 mM imidazole for 7 column volumes at 3 mL min^{-1}. The elution was continued at 500 mM imidazole for 2 column volumes to make sure bound proteins were all eluted. Collected fractions were concentrated to less than 2 mL by ulrafiltration (Millipore). Desalting experiment was carried out with HiTrap Desalting column × 5 (GE Healthcare) at 2 mL min^{-1}. Protein concentration was measured by BCA Protein Assay Kit.

Activity assay

The hydroxylation activity of PHD3 was detected *via* the fluorescence-based method which was developed by McNeill,[44]

based on reported derivatization methods for 2OG using *o*-phe-nylenediamine (OPD) to give a fluorescent derivative.[66] The assay of PHD3 activity was carried out by mixing 1 mM DTT, 0.6 mg mL^{-1} catalase, 2 mM ascorbate, 2 mg mL^{-1} BSA, 50 μM $FeCl_2$ (prepared as 500 mM stock in 20 mM HCl and diluted with water), HIF 19 peptide, enzyme and 20 mM PBS, pH 7.0, to a final volume of 96 μL, keeping on ice bath. The reaction was initiated by addition of 4 μL 2OG (160 μM) to the reaction mixture. The details of the reaction procedure were listed in the ESI† (Experimental details). After activity and derivatization assay, quantitative analysis of the concentration of remained 2OG after the catalytic reaction was carried out from the maximum response of the fluorescence intensity of the derivatization product between 2OG and OPD. Scanning emission and excitation spectra were recorded on a Perkin-Elmer spectrometer with the excitation filter at 340 nm and the emission filter at 420 nm.

Circular dichroism measurements and secondary structure analysis

CD (200–250 nm) spectra were recorded on a JASCO-J810 spectropolarimeter (Jasco Co., Japan) in a cell of 1 mm slit width and 10 mm light length. The scanning rate was set at 50 nm min^{-1}. The spectra were the average of twice readings. Standard measurements were carried out at room temperature in very dilute enzyme solutions (4 μM, pH 7.0). A blank spectrum of buffer was collected previously and the subtraction was automatically carried out to get the protein spectrum. The secondary structure contents of PHD3 were estimated with the Jasco secondary structure manager software using the reference CD data-Yang. Jwr.[50] β-sheet contents were recalculated through an empirical equation between α-helix and β-sheet contents.[51]

PHD3 fluorescence measurement for ligand binding

The protein fluorescence emission spectra were recorded in a Thermo Scientific Varioskan Flash at the excitation wavelength of 280 nm with a 96-well black plate at step size of 1 nm. The initial volume of each test protein solution was 100 μL. The slit widths on the excitation monochromators was 12 nm. All measurement was performed at 37 °C. The fluorescence was measured by titrating PHD3 (2 μM) and Fe^{2+} (50 μM) mixture in 50 mM PBS (pH 7.0) with increasing amounts of tetraazamacro-cycles in a concentration range of 10^{-4}–10^{-3} M. A blank spectrum of water was collected simultaneously.

Computational details

The ground state structure of the complex of **4**-iron and residues of first coordination shell of PHD3 active site was computed utilizing the density functional theory (DFT) method with the hybrid density functional Becke-3-Lee-Yang-Parr (B3LYP). Double valence 3–21 g basis set was used to nonmetal elements (C, H, N, S, and O), which reasonably balances the computational cost and the reliability of the results.[40] An effective core potential LanL2DZ basis set was defined for Fe to incorporate

the relativistic corrections. All of the theoretical calculations were carried out using the Gaussian98 program package.[67]

The quantum mechanical calculations performed to clarify the reaction mechanism of 2OG-dependent non-heme enzymes were described before.[62] A simplified model based on the crystal structure of the catalytic domain of PHD2–Fe^{2+}–UN9 (UN9, a biologically active 2OG analogous inhibitor) was constructed. In the model used in the calculations, the UN9 molecule was displaced by inhibitor **4**. Compared with the crystal structure, the model was composed of a ferrous ion together with groups modeling the most relevant first coordination shell ligands.[68] Specifically, histidines were modeled by imidazole rings, aspartic acid by acetate. In order to prevent unrealistic geometry changes during the geometry optimizations, some constraints were imposed on the residues. More specifically, the atoms marked with an asterisk in Figure were fixed to their positions in the X-ray structure. This procedure guarantees that the optimized structures have reasonable geometries.

Acknowledgements

Notes and references

1 C. J. Schofield and P. J. Ratcliffe, *Nat. Rev. Mol. Cell Biol.*, 2004, **5**, 343–354.
2 G. L. Semenza, *Trends Mol. Med.*, 2001, **7**, 345–350.
3 C. W. Pugh and P. J. Ratcliffe, *Nat. Med.*, 2003, **9**, 677–684.
4 R. K. Bruick and S. L. McKnight, *Science*, 2001, **294**, 1337–1340.
5 C. J. Schofield and Z. H. Zhang, *Curr. Opin. Struct. Biol.*, 1999, **9**, 722–731.
6 I. J. Clifton, L. C. Hsueh, J. E. Baldwin, K. Harlos and C. J. Schofield, *Eur. J. Biochem.*, 2001, **268**, 6625–6636.
7 W. G. Kaelin and P. J. Ratcliffe, *Mol. Cell*, 2008, **30**, 393–402.
8 K. S. Hewitson, L. A. McNeill and C. J. Schofield, *Curr. Pharm. Des.*, 2004, **10**, 821–833.
9 I. Melnikova, *Nat. Rev. Drug Discovery*, 2006, **5**, 627–628.
10 N. C. Warshakoon, S. D. Wu, A. Boyer, R. Kawamoto, J. Sheville, S. Renock, K. Xu, M. Pokross, A. G. Evdokimov, R. Walter and M. Mekel, *Bioorg. Med. Chem. Lett.*, 2006, **16**, 5598–5601.
11 N. C. Warshakoon, S. D. Wu, A. Boyer, R. Kawamoto, J. Sheville, S. Renock, K. Xu, M. Pokross, S. Zhou, C. Winter, R. Walter, M. Mekel and A. G. Evdokimov, *Bioorg. Med. Chem. Lett.*, 2006, **16**, 5517–5522.
12 M. Frohn, V. Viswanadhan, A. J. Pickrell, J. E. Golden, K. M. Muller, R. W. Burli, G. Biddlecome, S. C. Yoder, N. Rogers, J. H. Dao, R. Hungate and J. R. Allen, *Bioorg. Med. Chem. Lett.*, 2008, **18**, 5023–5026.
13 D. J. Prockop and K. I. Kivirikko, *J. Biol. Chem.*, 1969, **244**, 4838–4842.
14 J. B. Cooper and J. E. Varner, *Plant Physiol.*, 1983, **73**, 324–328.
15 K. L. Gorres, R. Edupuganti, G. R. Krow and R. T. Raines, *Biochemistry*, 2008, **47**, 9447–9455.
16 J. Mecinovic, C. Loenarz, R. Chowdhury and C. J. Schofield, *Bioorg. Med. Chem. Lett.*, 2009, **19**, 6192–6195.
17 D. R. Mole, I. Schlemminger, L. A. McNeill, K. S. Hewitson, C. W. Pugh, P. J. Ratcliffe and C. J. Schofield, *Bioorg. Med. Chem. Lett.*, 2003, **13**, 2677–2680.
18 I. Schlemminger, D. R. Mole, L. A. McNeill, A. Dhanda, K. S. Hewitson, Y. M. Tian, P. J. Ratcliffe, C. W. Pugh and C. J. Schofield, *Bioorg. Med. Chem. Lett.*, 2003, **13**, 1451–1454.
19 M. A. McDonough, L. A. McNeill, M. Tilliet, C. A. Papamicael, Q. Y. Chen, B. Banerji, K. S. Hewitson and C. J. Schofield, *J. Am. Chem. Soc.*, 2005, **127**, 7680–7681.
20 C. J. Cunliffe, T. J. Franklin, N. J. Hales and G. B. Hill, *J. Med. Chem.*, 1992, **35**, 2652–2658.
21 M. A. McDonough, V. Li, E. Flashman, R. Chowdhury, C. Mohr, B. M. R. Lienard, J. Zondlo, N. J. Oldham, I. J. Clifton, J. Lewis, L. A. McNeill, R. J. M. Kurzeja, K. S. Hewitson, E. Yang, S. Jordan, R. S. Syed and C. J. Schofield, *Proc. Natl. Acad. Sci. U. S. A.*, 2006, **103**, 9814–9819.
22 P. Koivunen, M. Hirsila, A. M. Remes, I. E. Hassinen, K. I. Kivirikko and J. Myllyharju, *J. Biol. Chem.*, 2006, **282**, 4524–4532.
23 I. Melnikova, *Nat. Rev. Drug Discovery*, 2006, **5**, 627–628.
24 A. Thalhammer, J. Mecinovic, C. Loenarz, A. Tumber, N. R. Rose, T. D. Heightman and C. J. Schofield, *Org. Biomol. Chem.*, 2011, **9**, 127–135.
25 H. Skarpos, D. V. Vorob'eva, S. N. Osipov, I. L. Odinets, E. Breuer and G.-V. Roschenthaler, *Org. Biomol. Chem.*, 2006, **4**, 3669–3674.
26 C. Salvarani, R. Baricchi, D. Lasagni, L. Boiardi, R. Piccinini, C. Brunati, P. Macchioni and I. Portioli, *Rheumatol. Int.*, 1996, **16**, 45–48.
27 S. Y. Yao, M. Soutto and S. Sriram, *J. Neurosci. Res.*, 2008, **86**, 2403–2413.
28 Y. Wu, X. Li, W. Xie, J. Jankovic, W. Le and T. Pan, *Neurochem. Int.*, 2010, **57**, 198–205.
29 O. Weinreb, T. Amit, S. Mandel, L. Kupershmidt and M. B. Youdim, *Antioxid. Redox Signaling*, 2010, **13**, 919–949.
30 A. L. Larroque, J. Dubois, S. Thoret, G. Aubert, A. Chiaroni, F. Gueritte and D. Guenard, *Bioorg. Med. Chem.*, 2007, **15**, 563–574.
31 G. J. Bridger, R. T. Skerlj, P. E. Hernandez-Abad, D. E. Bogucki, Z. Wang, Y. Zhou, S. Nan, E. M. Boehringer, T. Wilson, J. Crawford, M. Metz, S. Hatse, K. Princen, E. De Clercq and D. Schols, *J. Med. Chem.*, 2010, **53**, 1250–1260.
32 F. Liang, S. Wan, Z. Li, X. Xiong, L. Yang, X. Zhou and C. Wu, *Curr. Med. Chem.*, 2006, **13**, 711–727.
33 K. Ariga and T. Kunitake, in *Supramolecular Chemistry-Fundamentals and Applications*, Springer, Berlin, 2006, ch. 2, pp. 18–21.
34 B. Frydman, S. Bhattacharya, A. Sarkar, K. Drandarov, S. Chesnov, A. Guggisberg, K. Popaj, S. Sergeyev, A. Yurdakul, M. Hesse, H. S. Basu and L. J. Marton, *J. Med. Chem.*, 2004, **47**, 1051–1059.
35 J.-H. Wen, C.-Y. Li, Z.-R. Geng, X.-Y. Ma and Z.-L. Wang, *Chem. Commun.*, 2011, **47**, 11330–11332.
36 I. Batinic-Haberle, J. S. Reboucas and I. Spasojevic, *Antioxid. Redox Signaling*, 2010, **13**, 877–918.
37 D. M. Kurtz, *J. Inorg. Biochem.*, 2006, **100**, 679–693.
38 M. S. Lah, M. M. Dixon, K. A. Pattridge, W. C. Stallings, J. A. Fee and M. L. Ludwig, *Biochemistry*, 1995, **34**, 1646–1660.
39 E. I. Solomon, A. Decker and N. Lehnert, *Proc. Natl. Acad. Sci. U. S. A.*, 2003, **100**, 3589–3594.
40 Z. Geng, J. Zhu, J. Cao, J. Geng, X. Song, Z. Zhang, N. Bian and Z. Wang, *J. Inorg. Biochem.*, 2011, **105**, 273–281.
41 G. Wulfsberg, in *Inorg. Chem.*, ed. J. Stiefel, University Science Books, Sausalito, 2000, ch. 5, pp. 191–225.
42 J. Wen, Z. Geng, Y. Yin and Z. Wang, *Dalton Trans.*, 2011, **40**, 9737–9745.
43 N. Fedulova, J. Hanrieder, J. Bergquist and L. O. Emren, *Protein Expression Purif.*, 2007, **54**, 1–10.
44 L. A. McNeill, L. Bethge, K. S. Hewitson and C. J. Schofield, *Anal. Biochem.*, 2005, **336**, 125–131.
45 H. Maumela, R. D. Hancock, L. Carlton, J. H. Reibenspies and K. P. Wainwright, *J. Am. Chem. Soc.*, 1995, **117**, 6698–6707.
46 T. S. Robinson, O. Wyness, S. F. Lincoln, M. R. Taylor, E. R. T. Tiekink and K. P. Wainwright, *Inorg. Chim. Acta*, 2006, **359**, 1413–1420.
47 W. W. Cleland, in *The Enzymes*, ed. D. S. Sigman and P. D. Boyer, Academic Press, San Diego, 3rd edn, 1990, vol. 19, ch. 3, pp. 99–155.
48 J. P. Hennessey Jr. and W. C. Johnson Jr., *Biochemistry*, 1981, **20**, 1085–1094.
49 W. C. Johnson, *Proteins*, 1990, **7**, 205–214.
50 J. T. Yang, C. S. Wu and H. M. Martinez, in *Methods in Enzymology*, ed. C. H. W. Hirs and S. N. Timasheff, Academic Press, Massachusetts, 1986, vol. 130, 208–269.
51 J. B. Siegel, W. E. Steinmetz and G. L. Long, *Anal. Biochem.*, 1980, **104**, 160–167.
52 R. Chowdhury, M. A. McDonough, J. Mecinovic, C. Loenarz, E. Flashman, K. S. Hewitson, C. Domene and C. J. Schofield, *Structure*, 2009, **17**, 981–989.
53 B. Bleijlevens, T. Shivarattan, E. Flashman, Y. Yang, P. J. Simpson, P. Koivisto, B. Sedgwick, C. J. Schofield and S. J. Matthews, *EMBO Rep.*, 2008, **9**, 872–877.

This journal is © The Royal Society of Chemistry 2012

54 C. J. Stubbs, C. Loenarz, J. Mecinovic, K. K. Yeoh, N. Hindley, B. M. Lienard, F. Sobott, C. J. Schofield and E. Flashman, *J. Med. Chem.*, 2009, **52**, 2799–2805.

55 A. V. Hill, *J. Physiol. (London, U. K.)*, 1910, **40**, iv–vii.

56 J. T. Vivian and P. R. Callis, *Biophys. J.*, 2001, **80**, 2093–2109.

57 K. Arnold, L. Bordoli, J. Kopp and T. Schwede, *Bioinformatics*, 2006, **22**, 195–201.

58 F. Kiefer, K. Arnold, M. Kunzli, L. Bordoli and T. Schwede, *Nucleic Acids Res.*, 2009, **37**, D387–D392.

59 M. C. Peitsch, *Bio-Technology*, 1995, **13**, 723–723.

60 J. D. Oliver, D. F. Mullica, B. B. Hutchinson and W. O. Milligan, *Inorg. Chem.*, 1980, **19**, 165–169.

61 G. L. Woolery, M. A. Walters, K. S. Suslick, L. S. Powers and T. G. Spiro, *J. Am. Chem. Soc.*, 1985, **107**, 2370–2373.

62 T. Borowski, A. Bassan and P. E. M. Siegbahn, *Chem.–Eur. J.*, 2004, **10**, 1031–1041.

63 T. Borowski, A. Bassan and P. E. Siegbahn, *Inorg. Chem.*, 2004, **43**, 3277–3291.

64 R. D. Hancock, M. Salim Shaikjee, S. M. Dobson and J. C. A. Boeyens, *Inorg. Chim. Acta*, 1988, **154**, 229–238.

65 K. O. A. Chin, J. R. Morrow, C. H. Lake and M. R. Churchill, *Inorg. Chem.*, 1994, **33**, 656–664.

66 J. Muhling, M. Fuchs, M. E. Campos, J. Gonter, J. M. Engel, A. Sablotzki, T. Menges, S. Weiss, M. G. Dehne, M. Krull and G. Hempelmann, *J. Chromatogr., B: Anal. Technol. Biomed. Life Sci.*, 2003, **789**, 383–392.

67 M. J. Frisch, G. W. Trucks, H. B. Schlegel, G. E. Scuseria, M. A. Robb, J. R. Cheeseman, J. A. Montgomery, T. Vreven, K. N. Kudin, J. C. Burant, J. M. Millam, S. S. Iyengar, J. Tomasi, V. Barone, B. Mennucci, M. Cossi, G. Scalmani, N. Rega, G. A. Petersson, H. Nakatsuji, M. Hada, M. Ehara, K. Toyota, R. Fukuda, J. Hasegawa, M. Ishida, T. Nakajima, Y. Honda, O. Kitao, H. Nakai, M. Klene, X. Li, J. E. Knox, H. P. Hratchian, J. B. Cross, V. Bakken, C. Adamo, J. Jaramillo, R. Gomperts, R. E. Stratmann, O. Yazyev, A. J. Austin, R. Cammi, C. Pomelli, J. W. Ochterski, P. Y. Ayala, K. Morokuma, G. A. Voth, P. Salvador, J. J. Dannenberg, V. G. Zakrzewski, S. Dapprich, A. D. Daniels, M. C. Strain, O. Farkas, D. K. Malick, A. D. Rabuck, K. Raghavachari, J. B. Foresman, J. V. Ortiz, A. G. Baboul, S. Clifford, J. Cioslowski, B. B. Stefanov, G. Liu, A. Liashenko, P. Piskorz, I. Komaromi, R. L. Martin, D. J. Fox, T. Keith, A. Laham, C. Y. Peng, A. Nanayakkara, M. Challacombe, P. M. W. Gill, B. Johnson, W. Chen, M. W. Wong, C. Gonzalez and J. A. Pople, *Gaussian 98, (Revision A.9)*, Gaussian Inc., Pittsburgh, PA, USA, 1998.

68 A. V. Nemukhin, B. L. Grigorenko, I. A. Topol and S. K. Burt, *Int. J. Quantum Chem.*, 2006, **106**, 2184–2190.

This journal is © The Royal Society of Chemistry 2012

Org. Biomol. Chem., 2012, **10**, 3913–3923 | 3923